Simulation of Eddy Current Rail Testing Data for Neural Networks

Alexander Friedrich[1]

1 BAM, Germnay, alexander.friedrich@bam.de

Abstract

The present work is part of the AIFRI project (Artificial Intelligence For Rail Inspection), where we and our project partners train a neural network for defect detection and classification. Our goal at BAM is to generate artificial ultrasound and eddy current training data for the A.I. This paper has an exploratory nature, where we focus on the simulation of eddy current signals for head check cracks, one of the most important rail surface defects. The goal of this paper is twofold. On the one hand, we present our general simulation setup. This includes geometric models for head check cracks with features like branching and direction change, a model for the HC10 rail testing probe, and the configuration of the Faraday simulation software.
On the other hand, we use the Faraday software to simulate eddy current testing signals with a strong focus on the influence of the damage depth on the signal, while differentiating between different crack geometries. Here, we observe an early saturation effect of the test signal at a damage depth of 2 mm (at a crack angle of 25° to the surface). That is about 2 mm earlier than we would expect from measurements at a crack angle of 90°. This behavior will be investigated further in a future paper.
Finally, we interpolate the simulated signals in a two-step curve fitting process. With these interpolations we may generate eddy current test signals for any damage depth within the simulated range.

KEYWORDS: Simulation, Eddy Current, Artificial Intelligence

1. Introduction

The present research is done for the AIFRI project (Artificial Intelligence For Rail Inspection), where we and our project partners train a neural network for defect detection and classification. Since the current testing data is unbalanced, insufficiently labeled and largely unverified we will supplement fused, simulated eddy current and ultrasonic testing data in form of a configurable digital twin.
For eddy current testing, one of the most important rail surface defects is the head check,

 https://doi.org/10.58286/28179

or rather head check fields. They are cracks on the gauge corner of the rail caused by rolling contact fatigue of the wheel-rail interaction. They need to be detected reliably and their dimensions need to be estimated from the test signal, since they can develop into very serious rail defects. See [4] for a short introduction to rail surface defects and [2] for a review of the principles of eddy current testing.
As the crack geometry can be quite complex (e.g. direction changes or branching, see [1, page 58 ff.]), estimating the crack dimensions from the sparse data of the rail testing setup is very difficult and verifying the estimates in a laboratory scale setup is cumbersome, which renders it unfeasible for labeling training data. Hence, we systematically investigate the influence of the crack depth on the signal shape, using different degrees of complexity for the head check model.

2. Method

For different head check models we construct a complex valued function $F(x,d)$, such that $F(\cdot,d)$ approximates the test signal for depth d, allowing us to generate artificial test signals for any depth. To that end, we construct a CAD model of a test body with a defect in FreeCAD [5]. We import the CAD model into Faraday [6], add a model of a HC10 eddy current probe, and move the probe across the test body in 1 mm steps solving the model and calculating the induced voltage in every step. This is the sampling rate used by the rail testing trains. Afterwards, the data is analyzed and fitted using custom Python code. We like to point out that a similar investigation has been performed in [3], though not with a rail specimen and only for slit defects.

2.1 Defect Geometry

We construct the crack geometry out of cylinders and cone like structures with a hexagonal base. This allows us to model complex crack geometries using building blocks without going into the details of fracture mechanics. In particular, we model branching and direction change, both of which are features observed in head checks. In figure 2 we see examples of crack bodies, which are to be removed from the test body, a rectangular cuboid. We build the parametrized CAD models in FreeCAD [5] using its API. The most relevant parameters include crack width and depth d, the surface angle α and the crack angle β. Unless stated otherwise we choose a crack width of 0.1 mm, a surface angle of 0° and crack angle of 25° - the average crack angle for head checks used for evaluation on the German rail network, see figure 1.

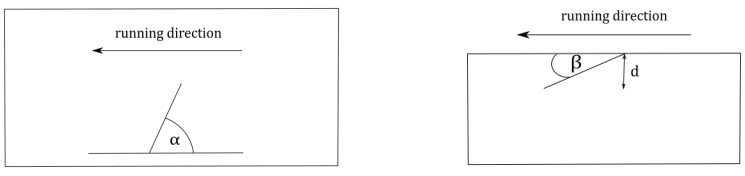

(a) Top view **(b) Side view**

Figure 1: Basic defect geometry

For branching cracks the angle of the branch can be specified. Here, we choose the angle such that the branch is parallel to the surface plane of the test body. For the direction

change the angle after the change can be specified. Here, we choose it such that the crack runs perpendicular to the surface plane.

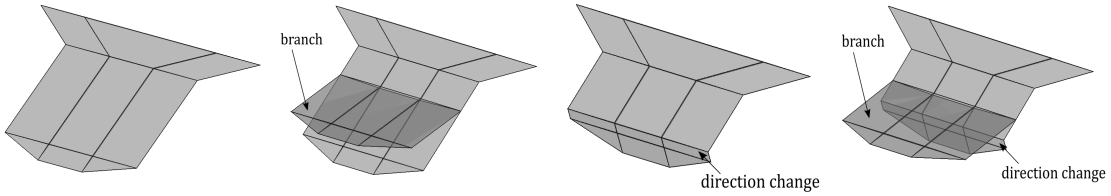

(a) Plain **(b) Branched** **(c) Direction change** **(d) Branched with direction change**

Figure 2: Examples of head check models.

2.2 Probe Geometry

We build a simplified model of the HC10 eddy current probe, see figure 3. The windings of the inner and outer coil have a ratio of $\frac{6}{25}$. In the simulation we assign a current of 1.2 A to the inner coil.

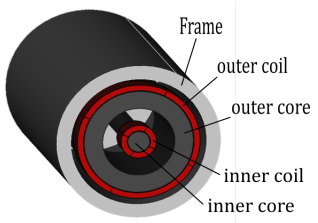

Figure 3: HC10 probe model

2.3 Simulation

We employ the Faraday software [6] using its BEM solver with 8000 to 9000 starting cells and 2 refinement steps, which each increase the number of cells by 25% according to internal criteria. We use the eddy current approximation, that is we disregard the displacement current in the simulation and use a time harmonic approach with a frequency of 150 kHz. The material parameters of the probe components where fitted and validated on measurements from our laboratory: $\mu_{core,inner} = 1328$, $\mu_{core,outer} = 1059$, $\mu_{frame} = 593$, $\sigma_{frame} = 1.507\,\mathrm{MS/m}$. Likewise, we determined the material parameters of the test body. We manufactured a specimen out of a piece of a used R65 rail and fitted the following parameters: $\mu_{body} = 29$, $\sigma_{body} = 1.182\,\mathrm{MS/m}$. We achieved a relative accuracy of 6.3 % (5.4 % for the imaginary part). We validated the fit with relative errors of at most 10% (6.7% for the imaginary part). While these errors are rather high, note that

- For eddy current testing the imaginary part of the test signal is usually rotated in the complex plane in such a way that the imaginary part is more pronounced and thus contains the more relevant defect information and the real part contains mostly information about the distance between probe and surface to be tested.
- We took several measurements for the specimen at different positions over the test slit and noticed that the some of the test signals differ significantly. For the real part we found relative errors up to 11%. We conjecture this is due to local changes in the material parameters, in particular the permeability.

2.4 Fitting and Interpolation

We normalize the signal such that the base line is at zero, meaning we seek to approximate compactly supported functions. The main idea is to fit modified Cauchy distributions to the real and imaginary parts of the signal. Denote the interval of depth parameter d by I_d and the interval of the position parameter x by I_x. For $x \in I_x$ and for the free parameters $a, h \in \mathbb{R}$, as well as $b, c, \alpha \in \mathbb{R}^+$, define

$$\begin{aligned} G_{a,b,c}(x) &:= \frac{c}{b^2 + (x-a)^2}, \\ \phi_\alpha(x) &:= \begin{cases} \exp\left(1 - \frac{1}{1-(x/\alpha)^2}\right) & \text{if } x < \alpha \\ 0 & \text{else} \end{cases}, \\ \tilde{F}(x) &:= \phi_\alpha(x)(h + G_{a,b,c}(x)). \end{aligned}$$

We employ the cutoff function ϕ_α since G is not compactly supported. First, we fit $\tilde{F}$ to the simulated signals, thus obtaining sets of parameters (a, b, c, α, h) for four to eight different depths, see figures 4, 5 and 6. Then, we fit polynomials and rational functions up to degree two to these parameters to obtain functions $a(d)$, etc. Finally, inserting these back into $\tilde{F}$ we obtain a function $F : I_x \times I_d \to \mathbb{R}$, where $F(\cdot, d)$ is the interpolated signal for any $d \in I_d$.

3. Results

In the following we understand depth d always as damage depth, that is normal to the specimen surface (see figure 1), since this is the quantity commonly used in rail testing. Since we investigate angled cracks, note that the crack depth d_{crack} is related to the damage depth d by $d_{crack} = d/\sin(\beta)$, where β is the crack angle. For $\beta = 25°$ we have $\sin(\beta)^{-1} \approx 2.4$. Additionally, for the sake of brevity, we will only present our results for the imaginary parts of the signals, as they are more relevant.

Figure 4a, shows the results of our simulation for a rectangular slit, with $\beta = 90°$. We clearly see the increase in signal height and a saturation effect at around $d = 6\,\text{mm}$ with increasing depth. This general behavior is expected but in measurements of slit test defects, on a test rail used for probe calibration, a saturation effect has been observed at 10 mm. We conjecture that this is due to the relatively large uncertainty in the fit for the material parameters. The fit of model parameters can likely be improved with a more selective meshing approach, and by using measurements from the above mentioned calibration rail since it has a larger variety of test defects then our current setup. We will investigate this as soon as the calibration rail is available to us.

Note that, since the defect geometry is symmetric around $x = 0$, we only simulated half of the signal to save time and completed the other half symmetrically.

Using the fitting procedure outlined in section 2.4 we find the function shown in figure 4b. It exhibits a mean relative normalized L^2 error with respect to the simulated signals of 2 %. That is, if we denote the set of depths where we have simulated signals by $\tilde{I}_d$, the simulated and interpolated signals for $d \in \tilde{I}_d$ by $s_{sim}(d)$ and $s_{int}(d)$, respectively, then we find $\underset{d \in \tilde{I}_d}{\text{avarage}} \left(\frac{||s_{sim}(d) - s_{int}(d)||_{L^2(I_x)}}{|I_x|(\max(s_{sim}(d)) - \min(s_{sim}(d)))} \right) = 0.02$.

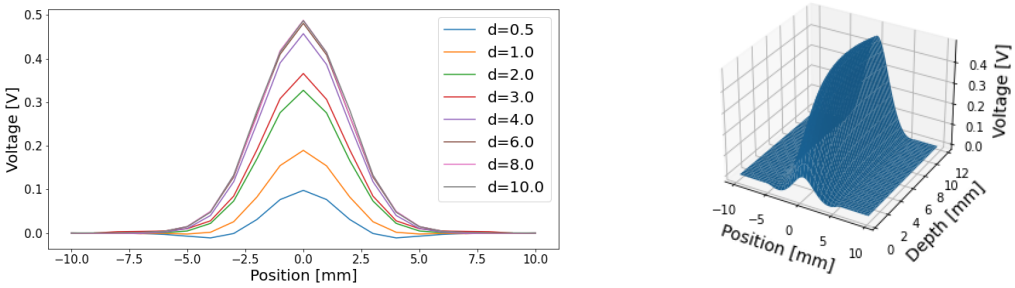

(a) Simulated signal **(b) Interpolated signal**

Figure 4: Depth dependency for a rectangular slit, $\beta = 90°$

Next we simulate and interpolate plain head checks and head checks with direction change at a crack angle of 25°. Figure 5 shows the results for the plain head check. We observe the same general behavior as before with saturation about $d = 2\,\text{mm}$. This corresponds to a crack depth of about 5 mm, which is consistent with our previous result. We observe this effect in our simulations with other head check types as well as with angled slits. After fitting, we find the functions shown in figures 5b and 6b. The interpolations show a mean relative normalized L^2 error with respect to the simulated signals of 5.1 % and 2.8 % for plain and direction change geometry respectively.

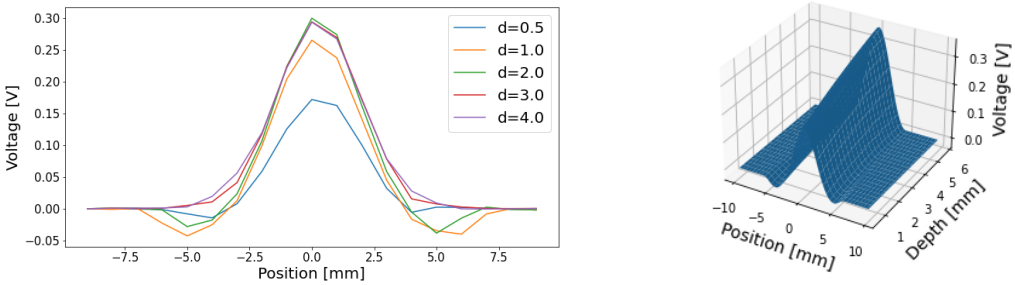

(a) Simulated signal **(b) Interpolated signal**

Figure 5: Depth dependency for the plain head check model, $\beta = 25°$

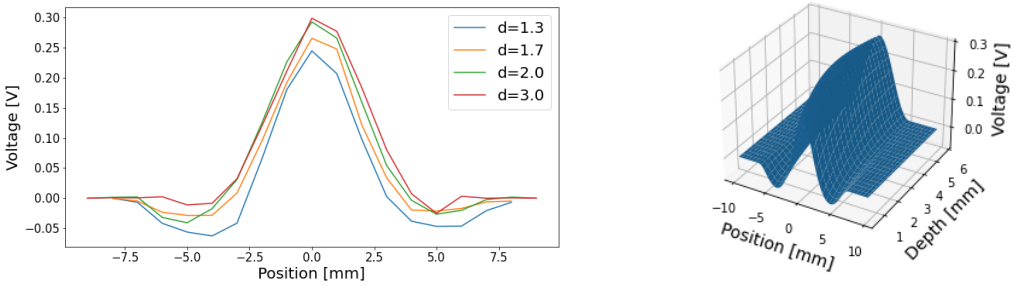

(a) Simulated signal **(b) Interpolated signal**

Figure 6: Depth dependency for the head check model with direction change, $\beta = 25°$

4. Conclusion

We present the construction of head check models in various degrees of complexity, the HC10 probe model and our simulation setup.
When analyzing the influence of the damage depth on the signal we see a clear increase in signal height until we reach saturation at about 6 mm and 2 mm depending on the crack angle. These thresholds are consistent with each other but inconsistent with measurements on other test bodies, where we have previously observed saturation at 10 mm.
Finally, the two step fitting process detailed in section 2.4 represents method to interpolate our simulated signals and obtain a signal for any depth between 0.5 mm and 4 mm for angled defects and any depth between 0.5 mm and 10 mm for vertical slits with satisfactory error estimates.

5. Outlook

An immediate continuation of the presented work is the further investigation of early saturation effect, using further simulations and validations with laboratory measurements to check our material parameter estimates and to rule out numerical errors. In order to estimate how reliable the defect depth can be determined for a given signal with noise, we will compare the signals of different head check models for varying depth and angles.
Finally, since we need to model head check fields for the AIFRI project, we will investigate if we can reliably approximate the total signal of closely neighboring head checks by their individual signals alone.

Acknowledgements

German Federal Ministry of Digital and Transport, mFUND (19FS2014)

References

[1] Karl-Otto Edel, Grigori Budnitzki, and Thomas Schnitzer. *Schienenfehler 1*. Springer Verlag, 2021.

[2] Javier García-Martín, Jaime Gómez-Gil, and Ernesto Vázquez-Sánchez. Non-destructive techniques based on eddy current testing. *Sensors*, 11(3):2525–2565, 2011.

[3] M. B. Kishore, J. W. Park, S. J. Song, H. J. Kim, and Se Gon Kwon. Characterization of defects on rail surface using eddy current technique. *Journal of Mechanical Science and Technology*, 33(9):4209–4215, 2019.

[4] Ishida Makoto. Rolling contact fatigue (rcf) defects of rails in japanese railways and its mitigation strategies. *Electronic Journal of Structural Engineering*, 13(1):67–74, 2013.

[5] Juergen Riegel, Werner Mayer, and Yorik van Havre. Freecad, version 0.19, 2023.

[6] INTEGRATED Engineering Software. Faraday, version 11.1, 2023.